Published by

OSA

®

The Optical Society

Tailored optical potentials for Cs atoms above waveguides with focusing dielectric nano-antenna

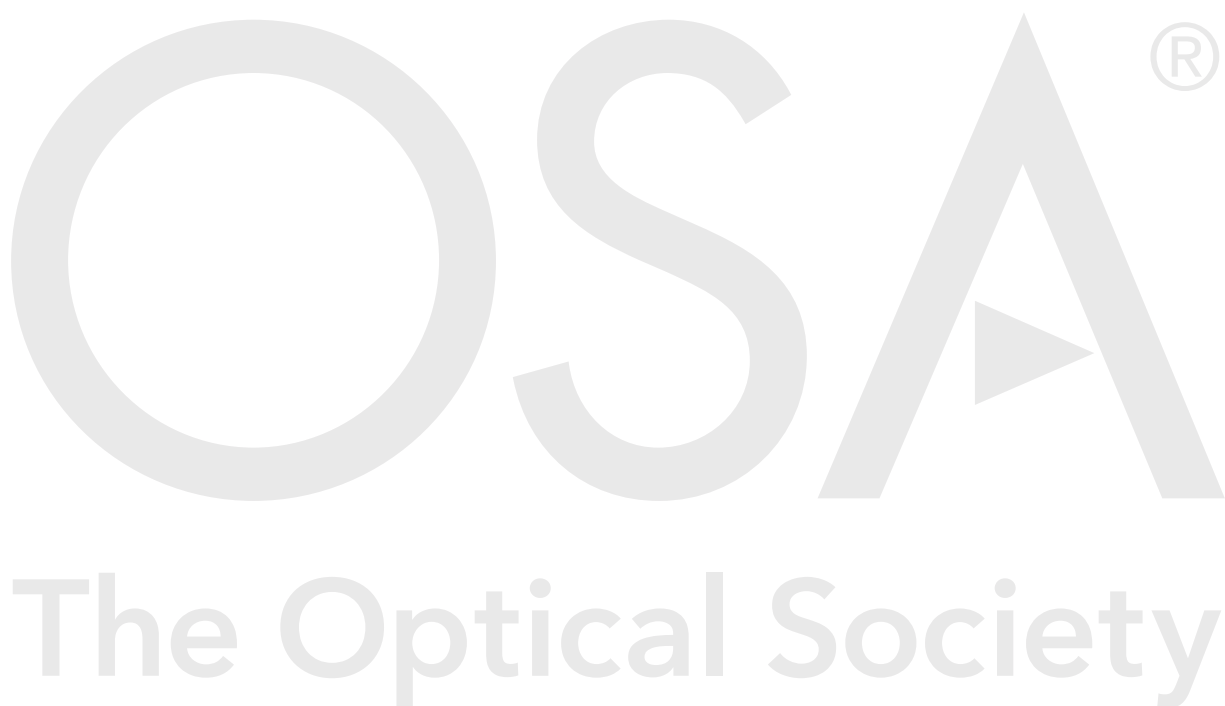ANGELEENE S. ANG[1,2†], ALEXANDER S. SHALIN[3], AND ALINA KARABCHEVSKY[1,2*]

[1] *School of Electrical and Computer Engineering, Ben-Gurion University of the Negev, Israel*
[2] *Center for quantum science and technology (BGU-QST), Ben-Gurion University of the Negev, Israel*
[3] *ITMO University, 49 Kronversky Ave., St. Petersburg, Russia*
*Corresponding author: alinak@bgu.ac.il
†Corresponding author: angeleene.ang@gmail.com

Tuning the near-field using all-dielectric nano-antennae offers a promising approach for trapping atoms, which could enable strong single-atom/photon coupling. Here we report the numerical study of an optical trapping of single Cs atom above a waveguide with silicon nano-antenna which produces a trapping potential for atoms in a chip-scale configuration. Using counter-propagating incident fields, bichromatically detuned from the atomic cesium D-lines, we numerically investigate the dependence of the optical potential on the nano-antenna geometry. We tailor the near-field potential landscape by tuning the evanescent field of the waveguide using a toroidal nano-antenna, a configuration that enables trapping of ultracold Cs atoms. Our research opens up a plethora of trapping atoms applications in a chip-scale manner from quantum computing to quantum sensing, to list a few. © 2020 Optical Society of America

Controlled positioning of atoms and molecules with extreme precision is a fascinating achievement in the field of quantum optics and photonics. Optical trapping was first shown by Ashkin in his seminal work (1970), where he trapped a dielectric microparticle (2018 Nobel Prize in Physics); in 1978, he suggested a three-dimensional trap for neutral atoms[1]. Since then, the optical trapping of particles and, specifically, atoms have been extensively investigated [2–4]. So far, the smallest optical atomic traps are realized with dimensions of half an optical wavelength. However, this is not a fundamental limit. Atomic trapping can be achieved at even smaller distances - in the sub-wavelength regime - by tuning near-fields in order to overcome the diffraction limit of far-fields.

In the case of confining a particle much smaller than the wavelength of the trapping light (Rayleigh regime), the trapping force is directly proportional to the intensity gradient of the field. High-power lasers have conventionally been used to generate a strong intensity gradient, for the trapping and manipulation of particles. To address the need for high laser power, optical
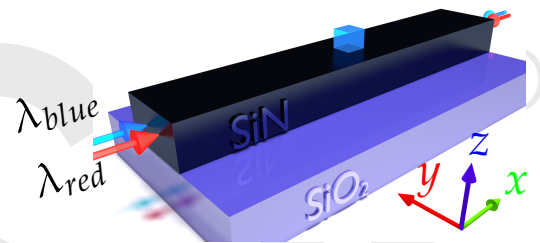

Fig. 1. Illustration of the studied all-optical atom trapping system with ridge waveguide, bi-chromatic incident light, and the silicon nano-antenna atop (not to scale).

trapping using plasmonic nanostructures or metamaterials[5] have been proposed, because plasmonic systems allow for localisation of an electromagnetic radiation at the nanoscale[6–11]. The plasmonic structures used in the aforementioned work are traditionally made of metals, which suffer from heating effects[12, 13], leading to Johnson noise, and limited storage time of atom-based systems[14, 15]. Previous works has, nevertheless, experimentally demonstrated atomic traps utilizing plasmonic structures[5, 16–18]. On the other hand, photonic nanojets - narrow, high-intensity light beams emerging from the shadow side of dielectric micro/nanostructures - generated by spheres embedded on top of a substrate illuminated by a plane wave, have been proposed as possible optical atomic traps[19, 20]. By removing the metallic element, an all-dielectric set-up greatly reduces the noise. Such systems, e.g., based on optical fibers[21–24], can provide electric fields sufficient for trapping a atoms.

Here, we propose an all-dielectric system concept for which the silicon nano-antennae is placed on top of a dielectric waveguide - as an alternative atomic trapping set-up to mitigate the heating issues while trapping atoms. For this, we numerically investigate the dependence of the bichromatically constructed trapping potentials for cesium atoms on the shape of the nano-antenna. Fig. (1) shows the schematics of the system we study: the counter-propagating incident bichromatic fields launched into both facets of the ridge waveguide to generate a standing wave for trapping along the propagation direction; the silicon nano-antenna placed on the waveguide to localize the light fur-

ther along the other directions.

To study the field focusing effect by different nano-antenna we calculate optical potentials produced by hemispherical, cubic, conical, toroidal, and hemielliptical nano-antenna geometries, as shown in Fig. (2). We note that the field focused by the nano-antenna, exhibit a global minimum of the optical potential, which corresponds to the presence of a stable atom trap. Unlike the conventional method of atom trapping with focused lasers, focusing with nanoantenna can easily be integrated into a miniaturized set-up. Unlike nanoplasmonic atomic lattices, the all-dielectric system proposed here is expected to reduce the harmful Johnson noise.
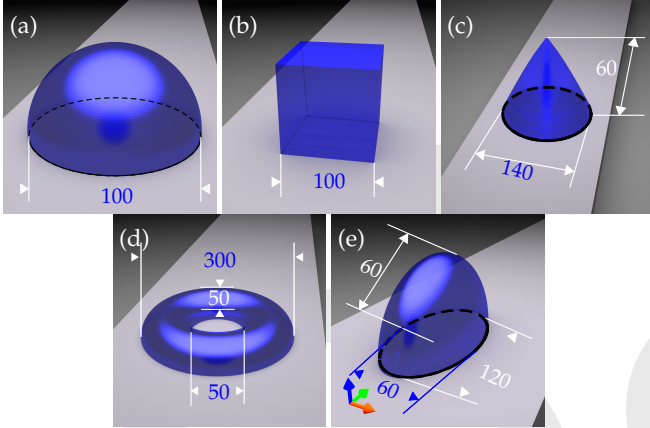

Fig. 2. The nano-antenna shapes and dimensions (all units in nm) considered for this paper (background not to scale).

Fiber-based atom traps are created by illuminating a glass fiber from both end-facets to form a standing wave that, in turn, generates a trapping potential[21–24], but this type of atom trap is limited to trapping atoms along a line. The configuration studied here also utilizes a standing wave and, as we discuss below, also enables the possibility of scalable traps in two dimensions. The trapping fields used in the fiber-based systems use two laser wavelengths, one which is red-detuned with respect to the atomic optical transition ($\lambda_{red} = 1094$ nm) to create an attractive light force, and the other being blue-detuned ($\lambda_{blue} = 652$ nm) to create a repulsive force. This is referred to as a bichromatic trapping system. The two fields together form an atom trap at the point where these forces are equal.

For linearly polarized incident light, each of these potentials is given by [2, 25]

$$U_{\text{opt},j} = \frac{\pi c^2 \Gamma}{2\omega_0^3} \left(\frac{1}{\omega_j - \omega_1} + \frac{2}{\omega_j - \omega_2} \right) I_{\text{opt},j}, \qquad \textbf{(1)}$$

where $I_{\text{opt},j}$ and ω_j are, respectively, the light intensity at the surface and frequency corresponding to the two light fields (j designating 'red' or 'blue'), and $\Gamma = 2\pi \times 5.2$ MHz and ω_0, respectively, are the natural linewidth and average transition frequency of the excited atomic levels in the D line of cesium. The transition frequencies are ω_1 and ω_2, where the subscript refers to the sublevels D_1 ($6^2S_{1/2} \to 6^2P_{1/2}$ with transition wavelength of 852.3 nm) and D_2 ($6^2S_{1/2} \to 6^2P_{3/2}$ with transition wavelength 894.6 nm) [26]. Calculating the bichromatic optical potential on an ordinary featureless ridge waveguide yields a series of minima spaced by half the optical wavelength along the propagation direction, which is similar to results obtained from related work on atomic trapping using optical fibers[21–24].

A sharp optical intensity gradient is required to generate strong localized forces. To produce this intensity gradient, we are introducing a perturbation in the boundary conditions, which, in this case, is the nano-antenna. We use silicon, a material with a high refractive index for VNIR (visible-near infrared) frequencies, in order to concentrate the energy from the waveguide at the near-field of the nano-antenna. In our system, the evanescent field's need to be more pronounced along the z axis (i.e., towards the cladding where an atom to be trapped), as opposed to the sides (i.e., along y), hence we use the fundamental TM mode for the input field[27]. As shown in Eq. (1), the optical potential is directly proportional to the field intensity, hence the optical potential can be written as[5, 25]

$$U_j(z) = U_{0j} \exp(-2z/z_{0j}), \qquad \textbf{(2)}$$

where U_{0j} is the potential strength at the surface and z_{0j} is the decay length of the evanescent wave. The potential dependence along x and y are calculated numerically. In order to take advantage of the evanescent wave's strong intensity gradient, the trap is designed such that the potential minimum is close to the surface.

We now consider an atomic trapping concept using nano-antennae on a planar waveguide, as the geometry of the waveguide would naturally allow multiple (scalable) trapping potentials either along its length (as a line of atoms) or in two dimensions (as an array of atoms) by adding more nano-antennae. Placing nano-antennae on top of the waveguide do not affect the guided modes. This conclusion is supported by the calculating the difference between the electric field magnitude with the nano-antenna ($|\mathbf{E}_{na}|$) and without ($|\mathbf{E}_{wg}|$), as shown in Fig. (3). This illustrates that the guiding layer is hardly perturbed by the presence of the nano-antenna; as can be seen, the maximum perturbation in the waveguide core, excluding the region near the nano-antenna is less than 10%. It is well-known that atomic lattices can be used as simulators to study strongly correlated quantum many-body systems[28]. By placing several nano-antennae in a 2D array one can explore the atom-atom and atom-photon interactions in more than one dimension.
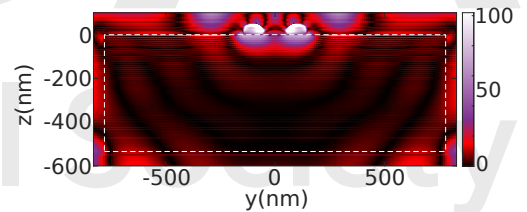

Fig. 3. Percent difference between the electric field magnitude in the waveguide without the nano-antenna ($|\mathbf{E}_{wg}|$) and with the nano-antenna ($|\mathbf{E}_{na}|$), calculated using $|(\mathbf{E}_{na} - \mathbf{E}_{wg})/\mathbf{E}_{na}|$. The dashed white rectangle indicates the boundaries of the guiding layer.

The silicon nitride (SiN) ridge waveguide on silica (SiO$_2$) substrate has dimensions of 1.56 μm along y and 0.534 μm along z to ensure 1) at least one confined quasi-TM mode; and 2) the evanescent tail of the fundamental TM mode allows for the sufficient penetration depth. Larger waveguides would excite the higher-order unnecessary modes modal interference effects. The fields were calculated using Lumerical FDTD, with the fundamental TM mode launched into the waveguide.

Sub-micron silicon nanostructures have been extensively studied in the field of all-dielectric resonators such as nanocubes,

nanocones and others[29]. Here we consider a cube and hemisphere for their simplicity in terms of fabrication[30]. In addition, to study nanoantenna characteristics that produce localized fields, we also consider a cone and a hemiellipse. Conical nanoantenna might provide better field localization in corners. The hemiellipse breaking symmetry might improve the field localization. To learn this, we show the total optical potential along Cartesian axises in Fig. (4) for those shapes. The sizes of the nano-antennae were selected to focus the fields on a sub-wavelength scale. We found that the sizes smaller than about $\lambda/6$ does not localize the fields sufficiently.

Table 1. Calculated numerical results with P_{red} and P_{blue} are the respective powers (in watts) of the field source for the red- and blue-detuned sources, z_d is the distance (in nm) from the potential minimum to the nano-antenna surface, U_0 indicates the optical potential minimum (in mK), U_{gs} is the zero-point energy (in mK), and U_{surf} is the estimated atom-surface potential (in mK).

Structure	P_{red}	P_{blue}	z_d	$U_{0,y}$	$U_{gs,z}$	U_{surf}
hemisphere	6.1	16.9	52	0.25	0.86	0.2
cube	6.1	16.2	43	0.53	1.07	0.4
cone	6.1	17.8	42	0.21	0.86	0.5
toroid	6.1	30.1	77	3.80	1.50	0.1
hemiellipse	6.1	15.6	36	1.13	1.36	0.7

More specific data from the simulations are shown in Table (1). We propose to illuminate the waveguide using the power scaling technique widely used in an integrated photonics: rare-earth dopants can be used on a segment of the waveguide to amplify the source to achieve the listed fields[31]. We note that the effects of nonlinearity can be neglected because the contribution of the nonlinear coefficient[32] reads as $Power \times 2.88 * 10^{-7}$, is negligible compared to the effective refractive index.

We consider two requirements before conclude that the potentials may be able to trap an atom. First, the optical trapping potential near its minimum must not be significantly perturbed by attractive atom-surface potentials that can destroy the trap near the surface. Second, the ground-state energy should lie within the potential well. We estimate the atom-surface potential U_{surf} using a Matlab code that calculates approximate Casimir-Polder and van der Waals potentials using the equations described in Sec III.B of Ref. [33], evaluated at $z = z_d$.

Table (1) compares U_{surf} to $U_{0,y}$ for each nano-antenna shape, where $U_{0,y}$ is the optical trapping potential along the y axis, i.e., the difference between the minimum and maximum of the curves shown in Fig. (4)c. Noting that the optical trapping force is dependent on the potential gradient, we see that this axis has the weakest trapping potential because of the shorter optical wavelength as compared to the width of the monomode waveguide. Table (1) also shows the ground-state energy $U_{gs,z}$ calculated assuming a harmonic potential along the z axis (here we use the z axis because it has the highest frequency $\omega_z > \omega_x > \omega_y$ and therefore gives the greatest contribution to the approximate 3D ground-state energy $U_{gs} = \hbar \left(\omega_x + \omega_y + \omega_z \right)/2$).

It is apparent from Table (1) that only the toroidal nano-antenna produces sufficiently strong potential along the y axis to support any bound states, i.e., the ground-state energy $U_{gs,z}$ exceeds $U_{0,y}$ for all the other shapes so they cannot support even

a single bound state. The uniquely successful toroidal shape was chosen as one of the nano-antenna geometries considered in our study based on a previous paper[34] that reports a similar nano-antenna geometry generating an equilibrium force at the midpoint. We also note that the cross-section of the field generated by the toroidal nano-antenna, shown in Figs. S10 and S11 of the supplementary materials, is qualitatively similar to that shown in Ref. [34]. The toroidal nano-antenna also exhibits the lowest atom-surface potential U_{surf} for any of the shapes considered, partially because we have deliberately increased the blue-detuned laser power to push the potential minimum a little further from the surface; as it is only a small fraction of the potential minimum at these distances, we do not consider U_{surf} further. In Fig. (5), we show an isopotential surface at the ground-state energy $U_{gs,z}$ for the toroidal nano-antenna. This isopotential surface is completely closed, indicating at least qualitatively that an atom could indeed be trapped by the optical potential generated near such a nano-antenna. This more demanding test eliminates other geometries that we considered. We conclude that the dilectric nanoantenna of highly symmetric toroidal shape is the most suitable for atom trapping on a chip. Breaking the symmetry, in the case of the hemiellipse, improves the trap parameters, but not sufficiently for generating a closed isosurface at the zero-point energy.

For future perspective, bringing the atoms to distances below 100 nm from the nano-antenna surface may allow exploration of Casimir-Polder and van-der-Waals forces for the nano-antenna shapes considered here. This is a challenging theoretical problem as well as an experimental one, since the nano-antenna shape affects these forces qualitatively as well as quantitatively. Future work would also need to take into account the fabrication tolerances. It would also be interesting to explore heating effects that may be generated in such systems, as well as other possible mechanisms that can cause atoms to escape from the trap.

The temperature-associated effects such as in ref[35] are the subject of our future work. We would emphasize, however, that the potential trap generated on top of our all-dielectric system is essentially generated by the evanescent fields of the waveguide. For such a waveguide, the power carried by the evanescent field is about 0.08 of the overall power launched into the waveguide[27], hence the cladding region of the waveguide does not experience significant heating.

In conclusion, we have presented an optical trapping concept in an all-dielectric system, where a silicon nano-antenna produces a trapping potential for atoms in a chip-scale configuration. We numerically explored the dependence of the bichromatically constructed trapping potential on the nano-antenna shape. Our results show that the near-field induced potential landscape can be tailored to sub-wavelength dimensions by manipulating the evanescent field using different nano-antenna geometries on top of the waveguide. We found that the dielectric toroidal nano-antenna generates an all-optical Cs atom trap directly above it. This trapping set-up can be used as a method for trapping an array of single atoms with the advantage of the simplicity in integration within a silicon photonic platform, thereby paving the way toward fascinating atom-photon applications on a chip.
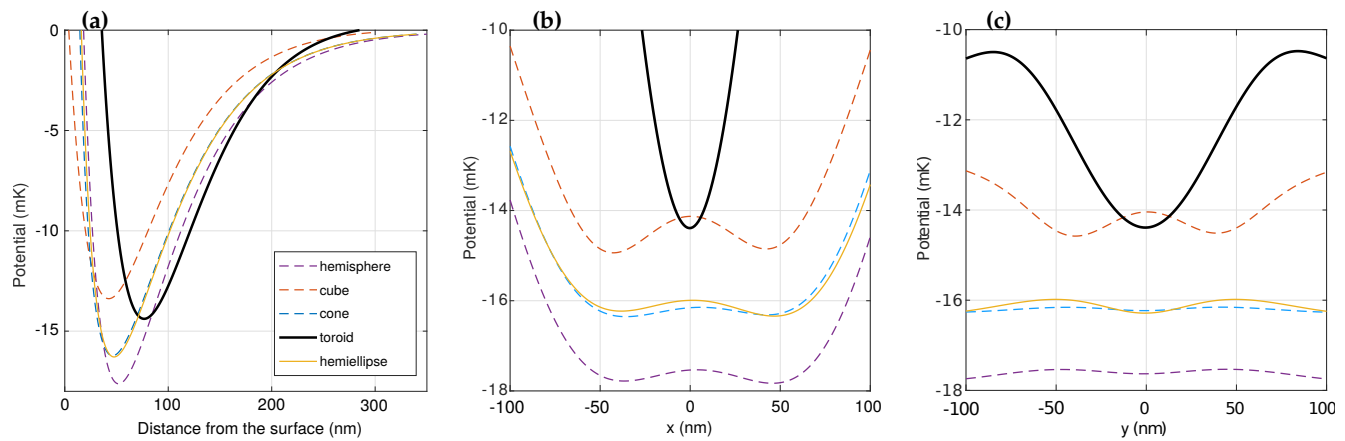
Fig. 4. Calculated (a) potential dependence on z where $x = y = 0$, (b) potential dependence on x where $z = z_d$ and $y = 0$, and (c) potential dependence on y where $z = z_d$ and $x = 0$. While these potential curves are useful for characterizing the potential minimum, the global potential minimum is better presented as a three-dimensional isosurface at a given energy (see Fig. 5).
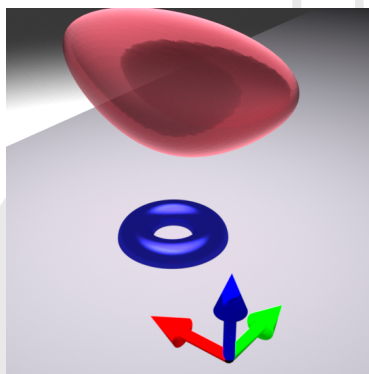

Fig. 5. Schematics of the potential isosurface at the zero-point energy for the toroidal nano-antenna. The isosurfaces for the remaining geometries are shown in Sec 5. of the Supplementary Materials.

REFERENCES

1. A. Ashkin, Phys. Rev. Lett. **40**, 729 (1978).
2. R. Grimm, M. Weidemüller, and Y. B. Ovchinnikov, "Optical Dipole Traps for Neutral Atoms," in *Advances In Atomic, Molecular, and Optical Physics,* , vol. 42 B. Bederson and H. Walther, eds. (Academic Press, 2000), pp. 95–170.
3. M. E. Kim, T.-H. Chang, B. M. Fields, C.-A. Chen, and C.-L. Hung, Nat Commun **10**, 1 (2019).
4. F. Nogrette, H. Labuhn, S. Ravets, D. Barredo, L. Béguin, A. Vernier, T. Lahaye, and A. Browaeys, Phys. Rev. X **4**, 021034 (2014).
5. C. Stehle, H. Bender, C. Zimmermann, D. Kern, M. Fleischer, and S. Slama, Nat. Photonics **5**, 494 (2011).
6. A. Karabchevsky, A. Mosayyebi, and A. V. Kavokin, Light. Sci. & Appl. **5**, e16164 (2016).
7. A. Karabchevsky, J. S. Wilkinson, and M. N. Zervas, Opt. express **23**, 14407 (2015).
8. A. Karabchevsky, O. Krasnykov, M. Auslender, B. Hadad, A. Goldner, and I. Abdulhalim, Plasmonics **4**, 281 (2009).
9. A. Karabchevsky, S. Karabchevsky, and I. Abdulhalim, Sensors Actuators B: Chem. **155**, 361 (2011).
10. A. Karabchevsky, I. Abdulhalim, C. Khare, and B. Rauschenbach, J. Nanophotonics **6**, 061508 (2012).
11. Y. Galutin, E. Falek, and A. Karabchevsky, Sci Rep **7**, 12076 (2017).
12. M. L. Brongersma and V. M. Shalaev, Science **328**, 440 (2010).
13. J. C. Ndukaife, V. M. Shalaev, and A. Boltasseva, Science **351**, 334 (2016).
14. M. E. Gehm, K. M. O'Hara, T. A. Savard, and J. E. Thomas, Phys. Rev. A **58**, 3914 (1998).
15. T. A. Savard, K. M. O'Hara, and J. E. Thomas, Phys. Rev. A **56**, R1095 (1997).
16. Z. Chen, F. Zhang, Q. Zhang, J. Ren, H. Hao, X. Duan, P. Zhang, T. Zhang, Y. Gu, and Q. Gong, Photon. Res. **5**, 436 (2017).
17. M. A. Zaman, P. Padhy, P. C. Hansen, and L. Hesselink, Appl. Phys. Lett. **112**, 091103 (2018).
18. Y. Tanaka, S. Kaneda, and K. Sasaki, Nano Lett. **13**, 2146 (2013).
19. V. Yannopapas, Opt. Commun. **285**, 2952 (2012).
20. V. Yannopapas and N. V. Vitanov, J. Phys.: Condens. Matter **21**, 245901 (2009).
21. H. L. Sørensen, J.-B. Béguin, K. W. Kluge, I. Iakoupov, A. S. Sørensen, J. H. Müller, E. S. Polzik, and J. Appel, Phys. Rev. Lett. **117**, 133604 (2016).
22. N. V. Corzo, B. Gouraud, A. Chandra, A. Goban, A. S. Sheremet, D. V. Kupriyanov, and J. Laurat, Phys. Rev. Lett. **117**, 133603 (2016).
23. E. Vetsch, D. Reitz, G. Sagué, R. Schmidt, S. T. Dawkins, and A. Rauschenbeutel, Phys. Rev. Lett. **104**, 203603 (2010).
24. A. Goban, K. S. Choi, D. J. Alton, D. Ding, C. Lacroûte, M. Pototschnig, T. Thiele, N. P. Stern, and H. J. Kimble, Phys. Rev. Lett. **109**, 033603 (2012).
25. M. Mildner, A. Horrer, M. Fleischer, C. Zimmermann, and S. Slama, J. Phys. B: At. Mol. Opt. Phys. **51**, 135005 (2018).
26. D. A. Steck, "Cesium D Line Data," (2003).
27. A. Katiyi and A. Karabchevsky, J. Light. Technol. **35**, 2902 (2017).
28. J. F. Sherson, C. Weitenberg, M. Endres, M. Cheneau, I. Bloch, and S. Kuhr, Nature. **467**, 68 (2010).
29. P. D. Terekhov, K. V. Baryshnikova, Y. A. Artemyev, A. Karabchevsky, A. S. Shalin, and A. B. Evlyukhin, Phys. Rev. B **96**, 035443 (2017).
30. P. D. Terekhov, K. V. Baryshnikova, Y. Greenberg, Y. H. Fu, A. B. Evlyukhin, A. S. Shalin, and A. Karabchevsky, Sci. reports **9**, 1 (2019).
31. C. R. Smith, S. J. Beecher, J. I. Mackenzie, and W. A. Clarkson, Appl. Phys. B **123**, 225 (2017).
32. K. Ikeda, R. E. Saperstein, N. Alic, and Y. Fainman, Opt. Express, OE **16**, 12987 (2008).
33. M. Rosenblit, Y. Japha, P. Horak, and R. Folman, Phys. Rev. A **73**, 063805 (2006).
34. Z. Xu and K. B. Crozier, Opt. Express **27**, 12 (2019).
35. M. Spector, A. Ang, O. Minin, I. Minin, and A. Karabchevsky, Nanoscale Adv. (2020).

FULL REFERENCES

1. A. Ashkin, "Trapping of Atoms by Resonance Radiation Pressure," Phys. Rev. Lett. **40**, 729–732 (1978).

2. R. Grimm, M. Weidemüller, and Y. B. Ovchinnikov, "Optical Dipole Traps for Neutral Atoms," in "Advances In Atomic, Molecular, and Optical Physics," , vol. 42, B. Bederson and H. Walther, eds. (Academic Press, 2000), pp. 95–170.

3. M. E. Kim, T.-H. Chang, B. M. Fields, C.-A. Chen, and C.-L. Hung, "Trapping single atoms on a nanophotonic circuit with configurable tweezer lattices," Nat Commun **10**, 1–8 (2019).

4. F. Nogrette, H. Labuhn, S. Ravets, D. Barredo, L. Béguin, A. Vernier, T. Lahaye, and A. Browaeys, "Single-Atom Trapping in Holographic 2D Arrays of Microtraps with Arbitrary Geometries," Phys. Rev. X **4**, 021034 (2014).

5. C. Stehle, H. Bender, C. Zimmermann, D. Kern, M. Fleischer, and S. Slama, "Plasmonically tailored micropotentials for ultracold atoms," Nature Photonics **5**, 494–498 (2011).

6. A. Karabchevsky, A. Mosayyebi, and A. V. Kavokin, "Tuning the chemi-luminescence of a luminol flow using plasmonic nanoparticles," Light: Science & Applications **5**, e16164 (2016).

7. A. Karabchevsky, J. S. Wilkinson, and M. N. Zervas, "Transmittance and surface intensity in 3d composite plasmonic waveguides," Optics express **23**, 14407–14423 (2015).

8. A. Karabchevsky, O. Krasnykov, M. Auslender, B. Hadad, A. Goldner, and I. Abdulhalim, "Theoretical and experimental investigation of enhanced transmission through periodic metal nanoslits for sensing in water environment," Plasmonics **4**, 281 (2009).

9. A. Karabchevsky, S. Karabchevsky, and I. Abdulhalim, "Fast surface plasmon resonance imaging sensor using radon transform," Sensors and Actuators B: Chemical **155**, 361–365 (2011).

10. A. Karabchevsky, I. Abdulhalim, C. Khare, and B. Rauschenbach, "Microspot sensing based on surface-enhanced fluorescence from nanosculptured thin films," Journal of Nanophotonics **6**, 061508 (2012).

11. Y. Galutin, E. Falek, and A. Karabchevsky, "Invisibility Cloaking Scheme by Evanescent Fields Distortion on Composite Plasmonic Waveguides with Si Nano-Spacer," Sci Rep **7**, 12076 (2017).

12. M. L. Brongersma and V. M. Shalaev, "The Case for Plasmonics," Science **328**, 440–441 (2010).

13. J. C. Ndukaife, V. M. Shalaev, and A. Boltasseva, "Plasmonics—turning loss into gain," Science **351**, 334–335 (2016).

14. M. E. Gehm, K. M. O'Hara, T. A. Savard, and J. E. Thomas, "Dynamics of noise-induced heating in atom traps," Phys. Rev. A **58**, 3914–3921 (1998).

15. T. A. Savard, K. M. O'Hara, and J. E. Thomas, "Laser-noise-induced heating in far-off resonance optical traps," Phys. Rev. A **56**, R1095–R1098 (1997).

16. Z. Chen, F. Zhang, Q. Zhang, J. Ren, H. Hao, X. Duan, P. Zhang, T. Zhang, Y. Gu, and Q. Gong, "Blue-detuned optical atom trapping in a compact plasmonic structure," Photon. Res. **5**, 436–440 (2017).

17. M. A. Zaman, P. Padhy, P. C. Hansen, and L. Hesselink, "Extracting the potential-well of a near-field optical trap using the Helmholtz-Hodge decomposition," Appl. Phys. Lett. **112**, 091103 (2018).

18. Y. Tanaka, S. Kaneda, and K. Sasaki, "Nanostructured Potential of Optical Trapping Using a Plasmonic Nanoblock Pair," Nano Lett. **13**, 2146–2150 (2013).

19. V. Yannopapas, "Photonic nanojets as three-dimensional optical atom traps: A theoretical study," Optics Communications **285**, 2952–2955 (2012).

20. V. Yannopapas and N. V. Vitanov, "All-optical nanotraps for atoms atop flat metamaterial lenses: A theoretical study," J. Phys.: Condens. Matter **21**, 245901 (2009).

21. H. L. Sørensen, J.-B. Béguin, K. W. Kluge, I. Iakoupov, A. S. Sørensen, J. H. Müller, E. S. Polzik, and J. Appel, "Coherent Backscattering of Light Off One-Dimensional Atomic Strings," Phys. Rev. Lett. **117**, 133604 (2016).

22. N. V. Corzo, B. Gouraud, A. Chandra, A. Goban, A. S. Sheremet, D. V. Kupriyanov, and J. Laurat, "Large Bragg Reflection from One-Dimensional Chains of Trapped Atoms Near a Nanoscale Waveguide,"

Phys. Rev. Lett. **117**, 133603 (2016).

23. E. Vetsch, D. Reitz, G. Sagué, R. Schmidt, S. T. Dawkins, and A. Rauschenbeutel, "Optical Interface Created by Laser-Cooled Atoms Trapped in the Evanescent Field Surrounding an Optical Nanofiber," Phys. Rev. Lett. **104**, 203603 (2010).

24. A. Goban, K. S. Choi, D. J. Alton, D. Ding, C. Lacroûte, M. Pototschnig, T. Thiele, N. P. Stern, and H. J. Kimble, "Demonstration of a State-Insensitive, Compensated Nanofiber Trap," Phys. Rev. Lett. **109**, 033603 (2012).

25. M. Mildner, A. Horrer, M. Fleischer, C. Zimmermann, and S. Slama, "Plasmonic trapping potentials for cold atoms," J. Phys. B: At. Mol. Opt. Phys. **51**, 135005 (2018).

26. D. A. Steck, "Cesium D Line Data," (2003).

27. A. Katiyi and A. Karabchevsky, "Figure of merit of all-dielectric waveguide structures for absorption overtone spectroscopy," J. Lightwave Technol. **35**, 2902–2908 (2017).

28. J. F. Sherson, C. Weitenberg, M. Endres, M. Cheneau, I. Bloch, and S. Kuhr, "Single-atom-resolved fluorescence imaging of an atomic Mott insulator," Nature **467**, 68–72 (2010).

29. P. D. Terekhov, K. V. Baryshnikova, Y. A. Artemyev, A. Karabchevsky, A. S. Shalin, and A. B. Evlyukhin, "Multipolar response of nonspherical silicon nanoparticles in the visible and near-infrared spectral ranges," Physical Review B **96**, 035443 (2017).

30. P. D. Terekhov, K. V. Baryshnikova, Y. Greenberg, Y. H. Fu, A. B. Evlyukhin, A. S. Shalin, and A. Karabchevsky, "Enhanced absorption in all-dielectric metasurfaces due to magnetic dipole excitation," Scientific reports **9**, 1–9 (2019).

31. C. R. Smith, S. J. Beecher, J. I. Mackenzie, and W. A. Clarkson, "Amplification of a radially polarised beam in an Yb:YAG thin-slab," Appl. Phys. B **123**, 225 (2017).

32. K. Ikeda, R. E. Saperstein, N. Alic, and Y. Fainman, "Thermal and Kerr nonlinear properties of plasma-deposited silicon nitride/silicon dioxide waveguides," Opt. Express, OE **16**, 12987–12994 (2008).

33. M. Rosenblit, Y. Japha, P. Horak, and R. Folman, "Simultaneous optical trapping and detection of atoms by microdisk resonators," Phys. Rev. A **73**, 063805 (2006).

34. Z. Xu and K. B. Crozier, "All-dielectric nanotweezers for trapping and observation of a single quantum dot," Opt. Express **27**, 12 (2019).

35. M. Spector, A. Ang, O. Minin, I. Minin, and A. Karabchevsky, "Temperature mediated'photonic hook'nanoparticle manipulator with pulsed illumination," Nanoscale Advances (2020).